Articles

Origin and Relevance of the Staggering in One-Dimensional "Molecular Metals". A Density Functional Study of Metallophthalocyanine Model Dimers

A. Rosa[†] and E. J. Baerends*

Theoretical Chemistry, Chemistry Department, Free University, De Boelelaan 1083, 1081 HV Amsterdam, The Netherlands

Received December 26, 1991

Electronic structure aspects of the interaction between the metallophthalocyanine units in the stacks forming a one-dimensional molecular metal are investigated for M(Pc)I (M = Co, Ni, Cu; Pc = phthalocyaninato; I is the dopant). Density functional calculations are carried out on the complete benzoporphyrin-like ring systems. An energy analysis in terms of electrostatic interaction, Pauli repulsion (steric hindrance), and occupied/virtual orbital interactions is presented. The following are concluded (a) The staggering angle of ~40° between adjacent rings originates from steric hindrance effects that can be traced to Pauli repulsion between occupied orbitals mainly located on the benzo rings. (b) The highest occupied π ligand orbital, $2a_{1u}$, forms the conduction band in the Ni and Cu systems. In the Co system the metal d_{z^2} plays a role. However, this system may not be a simple metal-spine conductor, but a two-band model (ligand π orbital ($2a_{1u}$) and metal d_{z^2} ($13a_{1g}$) bands) might be more appropriate. (c) The overlap between neighboring $2a_{1u}$ orbitals is zero at ~22°. The overlap (Pauli) repulsion of the $2a_{1u}$ orbitals would therefore drive the system to ~22°, at which angle the conductivity would be small. The steric hindrance of the benzo rings however is stronger and drives the angle to ~40°, where the dispersion of the $2a_{1u}$ band and therefore the conductivity is considerable. The benzo rings therefore play a key role in the conductivity. (d) The oxidation (doping) removes electrons from the top of the $2a_{1u}$ band and, apart from creating holes to act as charge carriers, relieves some of the $2a_{1u}$ repulsion present at ~40°, facilitating the change from slipped to metal-over-metal stacking.

Introduction

The one-dimensional "molecular metals" that contain partially oxidized porphyrin metallomacrocycles as molecular building blocks are receiving considerable interest.[1-4] The chemical flexibility inherent in the porphyrin-like metallomacrocycle provides a unique opportunity to vary the electronic structure through ligand and metal modification and allows for a systematic correlation of these modifications with the changes induced in several crucial attributes of the conductive molecular assemblies. Previous experience has shown that chemical or electrochemical oxidation changes significantly the structural features of these systems. The undoped porphyrin metallomacrocycles present a stacking pattern (**1a**) in which the neighboring rings are slipped

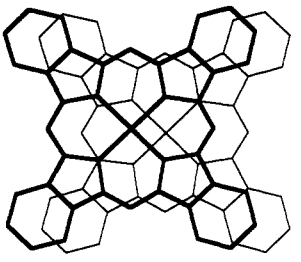

1a

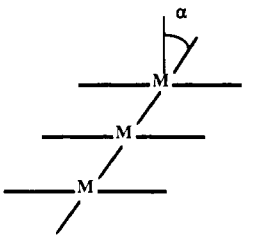

1b

and the α angle formed between the molecular symmetry axis and the stacking direction (**1b**) ranges in MPc's (where instead of Pc we may also have tbp, tatbp, tmp, omtbp, etc.[5]) from ~26 to ~45°, depending on their polymorphic form.[6,7] The doped compounds crystallize instead in the form of metal-over-metal columnar stacks (**2a**) of partially oxidized units surrounded by chains of anions. [The anions are actually $(I_3)^-$ units, so these compounds should perhaps be written $M(Pc)(I_3)_{1/3}$, but we will stick to the conventional notation M(Pc)I]. Successive rings in the stacks assume a staggered conformation with a rotation angle $\phi \approx 40°$ (**2b**) in virtually all large-ring benzoporphyrin-based

[†] Permanent address: Università degli Studi della Basilicata, Dipartimento di Chimica, Potenza, Italia.

(1) (a) Ibers, J. A.; Pace, L. J.; Martinsen, J.; Hoffman, B. M. *Struct. Bonding (Berlin)* **1982**, *50*, 1–55. (b) Ferraro, J. R. *Coord. Chem. Rev.* **1982**, *43*, 205–232. (c) Hoffman, B. M.; Ibers, J. A. *Acc. Chem. Res.* **1983**, *16*, 15–21. (d) Proceedings of the International Conference on the Physics and Chemistry of Low Dimensional Synthetic Metals (ICSM 84). *Mol. Cryst. Liq. Cryst.* **1985**, *120*. (e) Martinsen, J.; Pace, L. J.; Phillips, T. E.; Hoffman, B. M.; Ibers, J. A. *J. Am. Chem. Soc.* **1982**, *104*, 83–91. (f) Hoffman, B. M.; Martinsen, J.; Pace, L. J.; Ibers, J. A. In *Extended Linear Chain Compounds*; Miller, J. S., Ed.; Plenum: New York, 1983; Vol. 3, pp 459–549. (g) Palmer, S. M.; Stanton, J. L.; Martinsen, J.; Ogawa, M. Y.; Heuer, W. B.; Van Wallendael, S. E.; Hoffman, B. M.; Ibers, J. A. *Mol. Cryst. Liq. Cryst.* **1985**, *125*, 1–11.

(2) (a) Schramm, C. J.; Stojakovic, D. R.; Hoffman, B. M.; Marks, T. J. *Science (Washington, D.C.)* **1978**, *200*, 47–48. (b) Schramm, C. J.; Scaringe, R. P.; Stojakovic, D. R.; Ibers, J. A.; Marks, T. J. *J. Am. Chem. Soc.* **1980**, *102*, 6702–6713. (c) Martinsen, J.; Green, R. L.; Palmer, S. M.; Hoffman, B. M. *J. Am. Chem. Soc.* **1983**, *105*, 677–678. (d) Martinsen, J.; Palmer, S. M.; Tanaka, J.; Green, R. L.; Hoffman, B. M. *Phys. Rev. B: Condens. Matter A* **1984**, *30*, 6269–6276. (e) Palmer, S. M.; Stanton, J. L.; Jaggi, N. K.; Hoffman, B. M.; Ibers, J. A.; Schwartz, L. H. *Inorg. Chem.* **1985**, *24*, 2040–2046. (f) Martinsen, J.; Stanton, J. L.; Green. R. L.; Tanaka, J.; Hoffman, B. M.; Ibers, J. A. *J. Am. Chem. Soc.* **1985**, *107*, 6915–6920. (g) Ogawa, M. Y.; Martinsen, J.; Palmer, S. M.; Stanton, J. L.; Tanaka, J.; Green, R. L.; Hoffman, B. M.; Ibers, J. A. *J. Am. Chem. Soc.* **1987**, *109*, 1115.

(3) (a) Phillips, T. E.; Scaringe, R. P.; Hoffman, B. M.; Ibers, J. A. *J. Am. Chem. Soc.* **1980**, *102*, 3435–3444. (b) Pace, L. J.; Martinsen, J.; Ulman, A.; Hoffman, B. M.; Ibers, J. A. *J. Am. Chem. Soc.* **1983**, *105*, 2612–2620. (c) Ogawa, M. Y.; Hoffman, B. M.; Lee, S.; Yadkowsky, M.; Halperin, W. P. *Phys. Rev. Lett.* **1986**, *57*, 1177–1180. (d) Liou, O.; Ogawa, M. Y.; Newcomb, T. P.; Quirion, J.; Lee, M.; Poirier, M.; Halperin, W. P.; Hoffman, B. M.; Ibers, J. A. *Inorg. Chem.* **1989**, *28*, 3889.

0020-1669/92/1331-4717$03.00/0

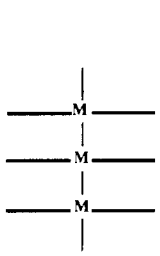

2a

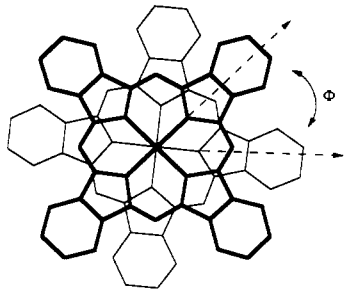

2b

conductors with an interplanar spacing not too different from the average value of 3.25 Å. For example, in the M(Pc)I series (M = Ni, Co, Cu, and "H_2")[1g] the rings are rotated by ~40° and in Ni(tbp)I[1e] and in Cu(tatbp)I,[3d] where the macrocyclic ligand is still phthalocyanine-like, the molecular units are staggered by 41 and 39.6°, respectively. In doped cofacially joined ($[M(Pc)O]I_x)_n$ polymers[8] (M = Si, Ge, Sn), the staggering angle changes from 39 to 40°, a very small amount, upon variation of the interplanar spacing as it occurs on going from M = Ge (3.48 Å) to M = Si (3.30 Å). There is one case, Ni(omtbp),[3a] where the staggering angle is exceptionally low: 26°. However, in this compound the macrocycle is "puckered" by intramolecular steric hindrance among the methyl groups with a resulting interplanar spacing of 3.78 Å, well beyond the average value of 3.25 Å found in other large-ring macrocyclic compounds.

The vast amount of experimental data available concerning the effects of the counterion on the stacking pattern of these conductors suggests that the size and structure of the oxidizing species, within a wide range of dimensions, has very little effect on the staggering angle of the donor units. For example in the crystals of Ni(Pc)Br[9] and in $([M(Pc)O]Br_x)_n$ polymers,[8] M = Si, Ge, Sn, the donor units exhibit the same staggering angle as in iodinated analogues. Furthermore, for a large number of counterions of different size and structure the degree of oxidation, $^1/_3$ electron/macrocycle ring, does not change. The degree of oxidation rather seems to be only a function of the crystal packing, as dictated by the donor units. This is in accord with studies[10] of metallophthalocyanine donors with dopants of different size and structure, such as TCNQ, DDQ, BF_4^-, and PF_6^-, where the maximum dopant level is invariably $\sim^1/_3$. However, there are examples where very large counterions induce radical modifications of the crystal packing and hence of the stoichiometry and degree of oxidation of the $[M(L)]_x[A]$ (L = macrocycle, A = counterion) class of molecular metals. Electrochemical oxidation of M(tatbp),[4b] M = Ni, Cu, in the presence of ReO_4^- affords a molecular crystal with three macrocycles in the cell and with a degree of oxidation $\sim^2/_3$. The M(tatbp) cations in a trimeric unit are staggered by 44.7°, which is only a minor deviation from the value ~40° found in M(tatbp)I.[3d] Another example where the anion size shows a large influence on the structure and stoichiometry of the conductors is the series of small-ring-based conductors Ni(tmp)I,[3b] $[Ni(tmp)]_2[PF_6]$,[4c] and $[M(tmp)]_2[ReO_4]$, M = Ni,[4c] Cu,[4f] Pd,[4g] where the staggering angle is 37, 34.7, and 27.5°, respectively, and the degree of oxidation which is $^1/_3$ in Ni(tmp)I becomes $^1/_2$ in $[Ni(tmp)]_2[PF_6]$ and $[Ni(tmp)]_2[ReO_4]$. A more careful inspection of the structural data concerning the above mentioned systems indicates that the main structural effect of the size of the counterion is its influence on the inter-ring distance. At a given inter-ring distance, however, the staggering angle is mostly related to the macrocycle features. The series $[M(tmp)]_2[ReO_4]$, M = Ni, Cu, Pd, where in all three systems the inter-ring separation is ~3.36 Å and the M(tmp) units are rotated by about the same angle of 27°, demonstrates the decisive effect of the given counterion (ReO_4) and macrocycle (tmp) on inter-ring distance and rotation angle, respectively. It can be concluded then that the counterion influences the staggering angle only indirectly, i.e. by determining the inter-ring distance.

That considerable experimental efforts have been made to gain insight in the peculiar stacking features of this class of molecular metals is not surprising in the light of the high sensitivity of the bandwidth and hence the conductivity to changes in the staggering angle, as shown by experimental and theoretical investigations.[3a,4e,10] To date however neither experimental studies nor theoretical investigations[11-13] have clarified the origin of the staggered conformation displayed by all oxidized porphyrin metallomacrocycles. Madelung energy calculations[11] that suggested a dependence of the rotation angle on the size of the counterion do not account for the experimentally observed angles.

As far as the electrical and magnetic properties are concerned, the conductors based on partially oxidized porphyrin metallomacrocycles show a variety of behaviors which are related to the nature of the metallic center as well as to the substituents on the porphyrin framework. Extensive experimental investigations suggest two pathways for the charge transport. The conductivity can originate from the interaction of neighboring π ligand orbitals, as in organic molecular metals, or the charge can propagate through metal-based orbitals, as in linear-chain spine conductors, owing to the occurrence of both metal d and ligand π interactions. There are also examples, for instance Ni(tbp)I,[1e] in which the charge carriers exhibit both metal and ligand properties. Among the metallomacrocycle-based conductors, the M(Pc)I series (M = Co, Ni, Cu) offers a unique, interesting example of the occurrence of these two limiting conductive behaviors. As a matter of fact, Ni(Pc)I[2b] and Cu(Pc)I[2g] display a charge transport through π ligand orbitals and in a wide range of temperature a metallic conductive behavior, in contrast Co(Pc)I[2f] has a semiconductor character and most likely is a metal-spine conductor. Thus, these electrical properties and the analogously peculiar magnetic behavior make Ni(Pc)I, Co(Pc)I, and Cu(Pc)I truly prototype systems.

(4) (a) Yakushi, K.; Sakuda, M.; Hamada, I.; Kuroda, H.; Kawamoto, A.; Tanaka, J.; Sugano, T.; Kinoshita, M. *Synth. Met.* **1987**, *19*, 769–774. (b) Almeida, M.; Kanatzidis, M. G.; Tonge, L. M.; Marks, T. J.; Marcy, H. O.; McCarthy, W. J.; Kannewurf, C. R. *Solid State Commun.* **1987**, *63*, 457–461. (c) Newcomb, T. P.; Godfrey, M. R.; Hoffman, B. M.; Ibers, J. A. *J. Am. Chem. Soc.* **1989**, *111*, 7078–7084. (d) Godfrey, M. R.; Newcomb, T. P.; Hoffman, B. M.; Ibers, J. A. *J. Am. Chem. Soc.* **1990**, *112*, 7260–7269. (e) Newcomb, T. P.; Godfrey, M. R.; Hoffman, B. M.; Ibers, J. A. *Inorg. Chem.* **1990**, *29*, 223–228. (f) McGhee, E. M.; Godfrey, M. R.; Hoffman, B. M.; Ibers, J. A. *Inorg. Chem.* **1991**, *30*, 803–808. (g) McGhee, E. M.; Hoffman, B. M.; Ibers, J. A. *Inorg. Chem.* **1991**, *30*, 2162–2165.

(5) Abbreviations used: pc, phthalocyaninato; omtbp, 1,4,5,8,9,12,13,16-octamethyltetrabenzoporphyrinato; tbp, tetrabenzoporphyrinato; tatbp, triazatetrabenzoporphyrinato; tmp, 5,10,15,20-tetramethylporphyrinato; TCNQ, 7,7,8,8-tetracyano-*p*-quinodimethane; DDQ,2,3-dichloro-5,6-dicyano-1,4-benzoquinone.

(6) (a) Honingmann, B.; Lenne, H.-U.; Schroedel, R. Z. *Kristallogr., Kristallogeom., Kristallphys., Kristallchem.* **1965**, *122*, 185. (b) Brown, C. J. *J. Chem. Soc. A* **1968**, 2494.

(7) (a) Brown, C. J. *J. Chem. Soc. A* **1968**, 2494. (b) Barret, P. A.; Dent, C. E.; Linstead, R. P. *J. Chem. Soc.* **1936**, 219. (c) Robertson, J. M.; Woodward, I. *Ibid.* **1937**, *219*. (d) Kirner, J. F.; Dow, W. *Inorg. Chem.* **1976**, *15*, 1685. (e) Scheidt, W. R.; Dow, W. *J. Am. Chem. Soc.* **1977**, *99*, 1101. (f) Mason, R.; Williams, G. A.; Fielding, P. E. *J. Chem. Soc., Dalton Trans.* **1979**, 676.

(8) Diel, B. N.; Inabe, T.; Lyding, J. W.; Schoch, K. F., Jr.; Kannewurf, C. R.; Marks, T. J. *J. Am. Chem. Soc.* **1983**, *105*, 1551.

(9) Palmer, S. M.; Stanton, J. L.; Hoffman, B. M.; Ibers, J. *Inorg. Chem.* **1986**, *25*, 2296.

(10) (a) Pietro, W. J.; Marks, T. J.; Ratner, M. A. *J. Am. Chem. Soc.* **1985**, *107*, 5387. (b) Konami, H.; Hatano, M.; Tajiri, A. *Chem. Phys. Lett.* **1990**, *166*, 605.

(11) Euler, W. B. *Inorg. Chem.* **1984**, *23*, 2645.

(12) (a) Canadell, E.; Alvarez, S. *Inorg. Chem.* **1984**, *23*, 573. (b) Whangbo, M.-H.; Stewart, K. R. *Isr. J. Chem.* **1983**, *23*, 133.

However, in spite of the vast amount of experimental data concerning these metallophthalocyanines, theoretical investigations, which mostly consist of semiempirical[12,13] or DV–Xα[14,15] calculations, are scarce, probably due to the large dimensions of these systems. These investigations have helped to rationalize the magnetic and electrical behavior of this class of conductors; however, they either do not deal with the origin and the influence on conductivity of the observed staggering or fail to account[12,13] for the experimental findings. Thus this question remains unsolved. Furthermore, we would like to stress that the failure of the Madelung energy calculations in predicting correctly the staggering angle points out[11] the inadequacy of an interpretation of the staggering purely in terms of electrostatic interactions.

In this paper we report a density functional study of the electronic structure of the prototype series of metallophthalocyanines Co(Pc)I, Ni(Pc)I, Cu(Pc)I. We address the following topics: (a) the origin and relevance of the staggering angle of $\sim$40° observed in MPc's as well as in most large-ring benzoporphyrin-based molecular metals; (b) the role of oxidation in the slipped to staggered configuration change and its importance for conductivity; (c) the nature of the carriers and the conduction pathways; (d) the origin of the different conductive behavior of Co(Pc)I with respect to Ni(Pc)I and Cu(Pc)I.

We will use, as fragments of the one-dimensional molecular stack, hypothetical dimeric metallomacrocycle moieties. This approach yields an adequate description of salient features of one-dimensional systems, as has been previously demonstrated.[10,16] Compared to band structure calculations, it renders unnecessary extreme simplifications to the ring structure in order to reduce computational effort. As we will see, retaining the full complexity of the large rings is crucial when one deals with the interactions between neighboring rings.

Computational and Methodological Details

The calculations reported in this paper were based on the LCAO density functional program system previously described.[17,18] A recently developed numerical integration scheme[19] allowed for the accurate and efficient evaluation of matrix elements appearing in the secular equation. Bonding energies were evaluated by the generalized transition-state method[20] and included Becke's nonlocal correction[21] to the local HFS exchange energy as well as Stoll's correction[22] for correlation between electrons of different spins, based on Vosko et al. parametrization[23] from electron gas data. It has been demonstrated that excellent metal–metal and metal–ligand bond energies are obtained from this density functional based approach.[24,25] The molecular orbitals were expanded in an uncontracted double-ζ STO basis set[26] for all atoms with the exception of the 3d metal orbital for which we used a triple-ζ STO basis set. For metal atoms we have added as polarization functions one 4p STO. The cores (Co, Ni, Cu: 1s2p; C,O: 1s) have been kept frozen.[17] The core orbitals have been taken from atomic calculations in a very large basis set, and in order to keep the valence levels orthogonal to these accurate cores the basis set has been augmented with a single STO for each atomic core orbital.[17] A set of auxiliary s, p, d, f, and g STO functions,[27] centered on all nuclei, was used to fit the molecular density and to generate the Coulomb and exchange potentials in each SCF cycle.

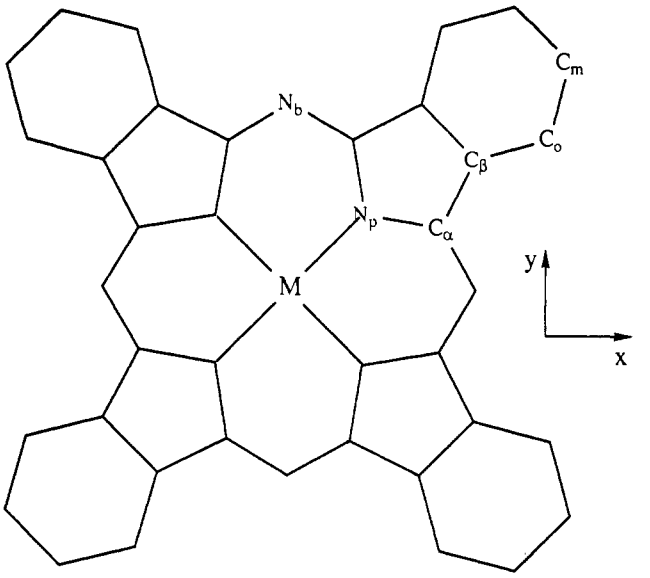

Figure 1. Atom-labeling scheme for phthalocyanine.

We have first performed calculations on CoPc, NiPc, and CuPc isolated molecules using the experimental geometry (see ref 2f, b, g, respectively), with appropriate averaging of bond angles and bond lengths to maintain the D_{4h} symmetry. The coordinate system used in the calculations as well as the labeling of the nonequivalent atomic centers in the ring is shown in Figure 1. The dimeric fragments have been built by superimposing, metal over metal, along the stacking direction (z axis in our coordinate system) two monomeric units at the interplanar distance they have in the molecular stack. This distance is 3.12,[2f] 3.24,[2b] and 3.19,[2g] Å in Co(Pc)I, Ni(Pc)I, and Cu(Pc)I, respectively.

In order to analyze the interactions between two neighboring molecules, for different staggering angles, we decompose the bonding energy into a number of terms. The first term, $\Delta E°$, is obtained from the energy of the wavefunction $\Psi°$ which is constructed as the antisymmetrized and renormalized product of the wavefunctions Ψ^A and Ψ^B of the fragments A and B:

$$\Psi° = NA\{\Psi^A\Psi^B\}$$

$$E° = \langle\Psi°|H|\Psi°\rangle,\ E^A = \langle\Psi^A|H^A|\Psi^A\rangle,\ E^B = \langle\Psi^B|H^B|\Psi^B\rangle$$

$$\Delta E° = E° - E^A - E^B = \Delta E_{\text{elstat}} + \Delta E_{\text{Pauli}}$$

$\Delta E°$, which is appropriately called the steric repulsion,[28,29] consists of two components. The first is the electrostatic interaction, ΔE_{elstat}, of the nuclear charges and unmodified electronic charge density of one fragment with those of the other fragment, both fragments being at their final positions. Usually, ΔE_{elstat} is negative, i.e. stabilizing. The second component is the so-called

(13) Bohm, M. C. *One-dimensional organometallic materials*; Lecture Notes in Chemistry, Springer Verlag: Berlin, 1987.
(14) Kutzler, F. W.; Ellis, D. E. *J. Chem. Phys.* **1986**, *84* (2), 1033.
(15) Liang, X. L.; Flores, S.; Ellis, D. E.; Hoffman, B. M.; Musselman, R. L. *J. Chem. Phys.* **1991**, *95*, 403.
(16) Ciliberto, E.; Doris, K. A.; Pietro, W. J.; Reisner, G. M.; Ellis, D. E.; Fragalà, I.; Herbstein, F. H.; Ratner, M. A.; Marks, T. J. *J. Am. Chem. Soc.* **1984**, *107*, 5387.
(17) Baerends, E. J.; Ellis, D. E.; Ros, P. *Chem. Phys.* **1973**, *2*, 42.
(18) Baerends, E. J.; Ros, P. *Int. J. Quantum Chem.* **1978**, *S12*, 169.
(19) Boerrigter, P. M.; te Velde, G.; Baerends, E. J. *Int. J. Quantum Chem.* **1988**, *33*, 87.
(20) Ziegler, T.; Rauk, A. *Theoret. Chim. Acta* **1977**, *46*, 1.
(21) Becke, A. D. *J. Chem. Phys.* **1986**, *84*, 4524.
(22) Stoll, H.; Golka, E.; Preuss, E. *Theor. Chim. Acta* **1980**, *29*, 55.
(23) Vosko, S. H.; Wilk, L.; Nusair, M. *J. Can. J. Phys.* **1980**, *58*, 1200.
(24) Ziegler, T.; Tschinke, V.; Becke, A. *Polyhedron* **1987**, *6*, 685.
(25) (a) Ziegler, T.; Tschinke, V.; Becke, A. *J. Am. Chem. Soc.* **1987**, *109*, 1351. (b) Ziegler, T.; Tschinke, V.; Ursenbach, C. *J. Am. Chem. Soc.* **1987**, *109*, 4825. (c) Ziegler, T.; Tschinke, V.; Versluis, L.; Baerends, E. J. *Polyhedron* **1988**, *7*, 1625.
(26) Snijders, J. G.; Vernooijs, P.; Baerends, E. J. *At. Data Nucl. Data Tables* **1982**, *26*, 483. Vermooijs, P.; Snijders, J. G.; Baerends, E. J. Slater type basis functions for the whole periodic system. Internal report; Vrije Universiteit: Amsterdam, 1981.
(27) Krijn, J.; Baerends, E. J. Fit functions in HFS-method. Internal report; Vrije Universiteit: Amsterdam, 1984 (in Dutch).
(28) Ziegler, T.; Rauk, A. *Inorg. Chem.* **1979**, *18*, 1558.
(29) Ziegler, T.; Rauk, A. *Inorg. Chem.* **1979**, *18*, 1755.

exchange repulsion or Pauli repulsion, ΔE_{Pauli}.[30,31] This is essentially due to the antisymmetry requirement on the total wavefunction, or equivalently the Pauli principle, which leads to a depletion of electron density in the region of overlap between Ψ^A and Ψ^B and an increase in kinetic energy.[32] It may be understood in a one-electron model as arising from the two-orbital four- or three-electron destabilizing interactions between occupied orbitals on the two fragments that form bonding and antibonding combinations that are *both* occupied. The repulsive effect is of course stronger the larger the overlap is between the two orbitals. It is therefore also referred to as overlap repulsion.

The Pauli repulsion due to the overlap of occupied bond orbitals or lone pair orbitals leads to the so-called steric hindrance effects, that, as we will see later, are responsible for the staggering of the neighboring rings observed in the investigated conductors. In this paper we will discuss quantitatively these steric hindrance effects.

In addition to the steric repulsion term $\Delta E°$, which is usually repulsive at the equilibrium distance since the repulsive component ΔE_{Pauli} dominates, there are the attractive orbital interactions which enter when the wavefunction $\Psi°$ is allowed to relax to the fully converged ground-state wavefunction of the total molecule, Ψ^{AB}. The energy lowering due to mixing of virtual orbitals of the fragments into the occupied orbitals is called the electronic interaction energy $\Delta E_{\text{int}} = E[\Psi^{AB}] - E°$. This term, according to the decomposition scheme proposed[28] by Ziegler, which is very useful for purposes of analysis, may be broken up into contributions from the orbital interactions within the various irreducible representations Γ of the overall symmetry group of the system:

$$\Delta E = \Delta E° + \Delta E_{\text{int}} = \Delta E° + \sum_{\Gamma} \Delta E(\Gamma)$$

Monomer Structure

The electronic structure of several metallophthalocyanines has already been investigated by a number of theoretical approaches,[15,33-38] and we will report elsewhere[39] a detailed study of the bonding in some first-row transition-metal phthalocyanines. However, as the nature of the interactions in the dimeric units depends on the character and energy of the MOs of the interacting monomers, we will briefly discuss here some aspects of the electronic structure of the isolated molecules. In Figure 2 the ground-state one-electron levels are shown for the series CoPc, NiPc, and CuPc, and for some selected molecular orbitals an atomic orbital population analysis is given in Table I. According to the occupation of the one-electron levels, the ground states of CoPc, NiPc, and CuPc are $^2A_{1g}$, $^1A_{1g}$, and $^2B_{2g}$, respectively.

Among the orbitals shown in Figure 2 and labeled according to D_{4h} notation, $11b_{2g}(d_{xy})$, doubly degenerate $6e_g(d_\pi)$ and $4e_g(d_\pi)$, $13a_{1g}(d_{z^2})$, and $8b_{1g}(d_{x^2-y^2})$ and $9b_{1g}(d_{x^2-y^2})$ involve the metal to a significant extent. It is noteworthy that these orbitals have quite different energies and compositions along the series, demonstrating the sensitivity of the electronic structure to changes in the relative Pc and metal energies. The $11b_{2g}$ orbital, which is empty except in CuPc where it contains the unpaired electron, is principally an antibonding M–N_p state composed of $3d_{xy}$ metal and pyrrolic nitrogen (N_p) lone pairs in almost equal amounts. Its bonding counterpart is much lower in energy because of the strong σ interaction. The energy gaps between $11b_{2g}$ and its bonding partner, $9b_{2g}$, not shown in the figure, are 6.87, 6.47, and 5.53 eV for CoPc, NiPc, and CuPc, respectively, indicating a weaker M–N_p interaction in CuPc. This is reasonable in view of the larger M–N_p bond length in CuPc (1.93 Å in CuPc vs 1.92 Å in CoPc and 1.87 Å in NiPc) and at the same time the smaller M–N_p overlap due to the contraction of the Cu $3d_{xy}$ orbital. The $13a_{1g}$ orbital whose energy is very sensitive to the nature of the metal, is mainly a pure metal orbital both in CoPc and NiPc, while in CuPc it shows accidentally a large participation of bridging nitrogen lone pairs. The d_{z^2} occurs in CuPc mostly (60%) in the $12a_{1g}$ that is almost degenerate with the $13a_{1g}$. The $6e_g$ orbital is heavily mixed with the p_z orbitals of the pyrrolic nitrogens; however the metal contribution decreases on going from CoPc to CuPc. Its bonding counterpart is the $4e_g$ orbital; $5e_g$ is instead a ligand orbital. We find the metal $d_{x^2-y^2}$ orbital, which points in our coordinate system to the bridging nitrogens, almost purely in the $8b_{1g}$ molecular orbital of NiPc and CuPc (78% and 92%, respectively). In CoPc, however, it is involved to the same extent in $8b_{1g}$ (47%) and $9b_{1g}$ (49%). The $d_{x^2-y^2}$ orbital has a π-in-plane interaction with the pyrrolic nitrogens, making the $8b_{1g}$ and $9b_{1g}$ molecular orbitals metal–Np bonding and antibonding, respectively.

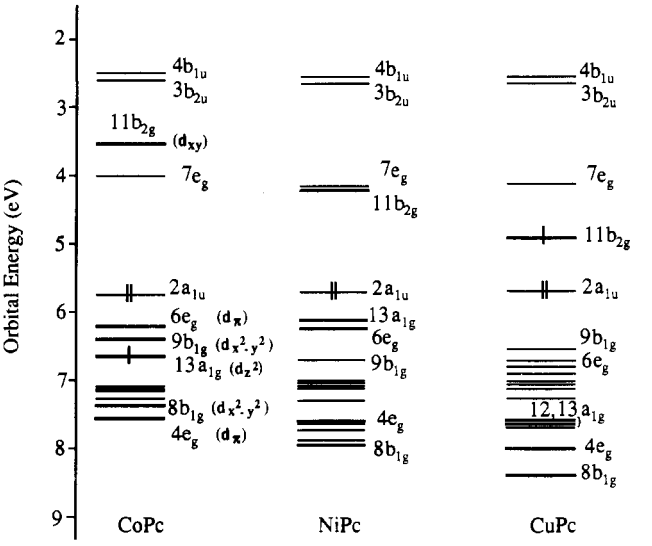

Figure 2. Energy levels scheme for the series of metallophthalocyanines. The labeled orbitals (heavy lines) are predominately of metal character.

From the level scheme of Figure 2 it may be inferred that the outstanding difference between the CoPc, NiPc, and CuPc molecules is the relative stabilization of the metal levels with respect to the ligand levels. For the latter we may take as a reference point $2a_{1u}$, which lies in all systems at the same energy and invariably is the highest *fully* occupied molecular orbital. For future reference we note that "unoccupied" $11b_{2g}$ has a diminishing gap with $2a_{1u}$ when going from Co to Cu (where it gets occupied with one electron). For the occupied metal states the downward shift when going from CoPc to CuPc is clearly distinguishable, but not uniform. The $13a_{1g}$ orbital is "anomalously" low in CoPc. This may be artificial, being related to its single occupancy in the CoPc ground state, a point to which we will return below. As will be seen in the next section, the relative positions of the occupied metal levels, notably the $13a_{1g}(d_{z^2})$, and the "unoccupied" metal level $11b_{2g}(d_{xy})$, with respect to the ligand $2a_{1u}$ are crucial for the properties of the molecular metals. The ligand $2a_{1u}$ orbital itself is known to be the main actor in the metallic behavior. For reference purposes a contour plot is given in Figure 4b, from which we note the nodal planes passing through

(30) Fujimoto, H.; Osamura, J.; Minato, T. *J. Am. Chem. Soc.* **1978**, *100*, 2954.
(31) Kitaura, K.; Morokuma, K. *Int. J. Quantum Chem.* **1976**, *10*, 325.
(32) van den Hoek, P. J.; Kleyn, A. W.; Baerends, E. J. *Comments At. Mol. Phys.* **1989**, *23*, 93.
(33) (a) Weiss, C.; Kobayashi, H.; Gouterman, M. *J. Mol. Spectrosc.* **1965**, *16*, 415. (b) McHugh, A.; Gouterman, M.; Weiss, C. *Theor. Chim. Acta (Berlin)* **1972**, *24*, 346. (c) Schaffer, A. M.; Gouterman, M.; Davidson, E. R. *Theor. Chim. Acta (Berlin)* **1973**, *30*, 9.
(34) Linder, R. E.; Rowlands, J. R. *Mol. Phys.* **1971**, *21*, 417.
(35) Chen, I.; Abkowitz, M.; Sharp, J. H. *J. Chem. Phys.* **1969**, *50*, 2237.
(36) (a) Mathur, S. C.; Singh, J. *Int. J. Quantum Chem.* **1972**, *6*, 57. (b) Mathur, S. C.; Singh, J. *Int. J. Quantum Chem.* **1974**, *8*, 79.
(37) Henriksson, A.; Roos, B.; Sundbom, M. *Theor. Chim. Acta (Berlin)* **1972**, *27*, 303.
(38) (a) Berkovitch-Yellin, Z.; Ellis, D. E. *J. Am. Chem. Soc.* **1981**, *103*, 6066. (b) Hale, P. D.; Pietro, W. J.; Ratner, M. A.; Ellis, D. E.; Marks, T. J. *J. Am. Chem. Soc.* **1987**, *109*, 5943.
(39) Rosa, A.; Baerends, E. J. Manuscript in preparation.

Table I. Percentage Contribution of Individual Atoms to Selected Orbitals (Based on Mulliken Population Analysis per MO) of Metallophthalocyanines with M = Co, Ni, and Cu[a]

		ε (eV)	M	N_p	C_α	C_β	N_b	C_o	C_m
$7e_g^*$	CoPc	−4.16	5.0 (d_π)	13.0	37.0	10.0	20.0	6.0	9.0
	NiPc	−4.17	4.8 (d_π)	13.0	38.2	11.0	19.0	5.0	9.0
	CuPc	−4.12	1.2 (d_π)	12.9	38.5	12.0	20.4	5.0	10.0
$11b_{2g}$	CoPc	−3.61	59.0 (d_{xy})	35.0 (lp)	2.0	4.0	0.0	0.0	0.0
	NiPc	−4.24	54.2 (d_{xy})	39.0 (lp)	3.0	4.0	0.0	0.0	0.0
	CuPc	−4.88	48.7 (d_{xy})	42.8 (lp)	3.2	5.3	0.0	0.0	0.0
$2a_{1u}$	CoPc	−5.74	0.0	0.0	58.5	1.2	0.0	26.5	13.8
	NiPc	−5.73	0.0	0.0	59.1	1.4	0.0	26.5	13.0
	CuPc	−5.67	0.0	0.0	59.7	1.3	0.0	25.0	14.0
$9b_{1g}$	CoPc	−6.41	49.1 ($d_{x^2-y^2}$)	5.0	4.6	3.2	38.1 (lp)	0.0	0.0
	NiPc	−6.70	18.9 ($d_{x^2-y^2}$)	9.0	6.0	2.8	63.0 (lp)	0.0	0.0
	CuPc	−6.53	4.0 ($d_{x^2-y^2}$)	11.2	5.8	2.7	75.9 (lp)	0.0	0.0
$6e_g$	CoPc	−6.24	61.7 (d_π)	6.6	6.8	11.2	0.0	3.4	10.3
	NiPc	−6.31	58.9 (d_π)	7.9	6.5	11.8	0.0	3.7	11.2
	CuPc	−6.71	14.8 (d_π)	20.5	1.0	29.6	1.1	2.8	30.2
$13a_{1g}$	CoPc	−6.64	96.7 (d_{z^2}, 4s)	3.3	0.0	0.0	0.0	0.0	0.0
	NiPc	−6.24	98.2 (d_{z^2}, 4s)	1.8	0.0	0.0	0.0	0.0	0.0
	CuPc	−7.60	37.4 (d_{z^2})	6.0	8.3	5.3	43.0	0.0	0.0
$4e_g$	CoPc	−7.55	24.7 (d_π)	8.1	4.0	22.4	0.5	5.3	35.0
	NiPc	−7.61	26.9 (d_π)	7.6	4.6	21.2	0.0	5.2	34.5
	CuPc	−8.04	60.0 (d_π)	0.5	11.0	6.3	0.0	6.3	15.9
$8b_{1g}$	CoPc	−7.35	47.0 ($d_{x^2-y^2}$)	5.8	4.5	0.0	42.7 (lp)	0.0	0.0
	NiPc	−7.93	77.0 ($d_{x^2-y^2}$)	2.2	3.9	0.0	16.9 (lp)	0.0	0.0
	CuPc	−8.50	92.0 ($d_{x^2-y^2}$)	0.6	2.9	0.0	4.5 (lp)	0.0	0.0

[a] On nitrogen and carbon the contributing AO's are $2p_z$, except for the $9b_{1g}$ and the $13a_{1g}$, in which they are mostly $2p_{x,y}$ with some 2s. The hydrogen contribution to these orbitals is almost negligible.

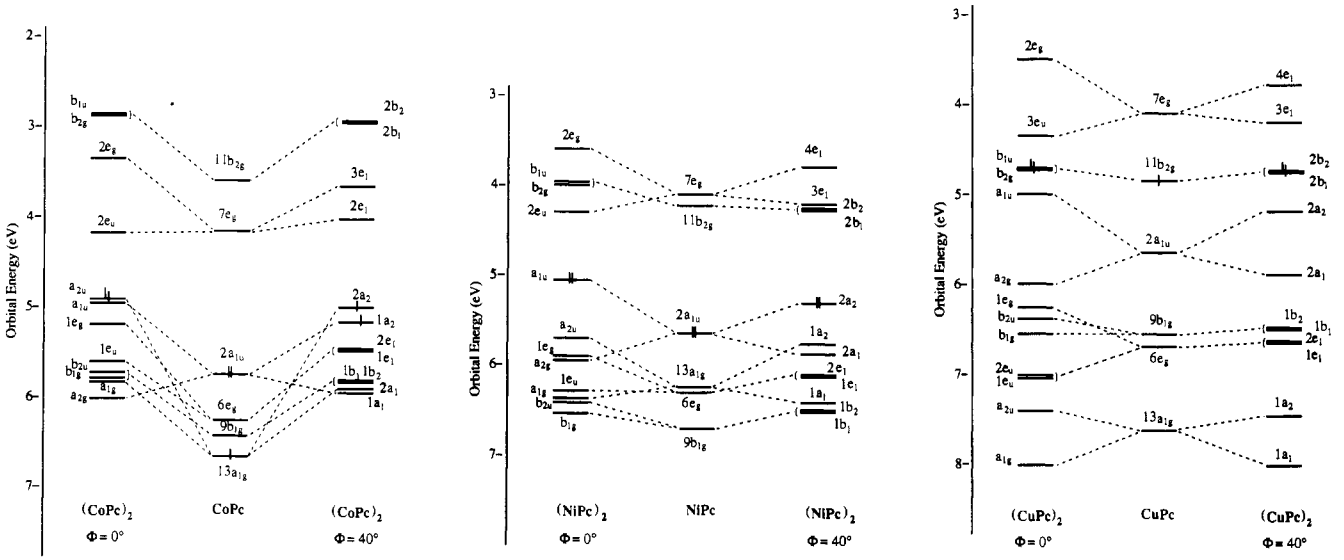

Figure 3. Orbital interaction diagrams for two metal over metal metallophthalocyanines in the eclipsed ($\phi = 0°$) and staggered ($\phi = 40°$) configuration: (a, left) interaction diagram for $(CoPc)_2$; (b, middle) interaction diagram for $(NiPc)_2$; (c, right) interaction diagram for $(CuPc)_2$.

both the pyrrolic and the bridging nitrogens and the strong contribution from the pyrrolic rings, notably the C_α atom.

Building up Dimers

(a) Orbital Interactions. The monomer orbitals are used to build up the molecular orbitals of $(CoPc)_2$, $(NiPc)_2$, and $(CuPc)_2$ dimers in the experimental staggered D_4 configuration ($\phi = 40°$) and in the idealized fully eclipsed D_{4h} configuration. The most important interactions are shown in the diagrams of Figure 3 for the three dimers in the two considered configurations. Let us look first at the nature and the origin of these interactions. For this purpose we report in Table II the overlap and the energy splitting of the most strongly interacting valence orbitals. As far as the metal states are concerned, the $13a_{1g}$ orbital, which is mainly d_{z^2} in the Co and Ni dimers, shows a significant broadening at all angles, which is quite obvious since we are considering a metal over metal stacking. The minor differences in the splitting of $13a_{1g}$ upon variation of the staggering angle are due to a slight mixing of other orbitals in the final dimer levels, which is only a second-order effect. The overlap and the energy gap between the $1a_1(a_{1g}$ in D_{4h} symmetry) bonding and the $1a_2(a_{2u}$ in D_{4h} symmetry) antibonding combinations of $13a_{1g}$ are largest in $(CoPc)_2$, as a consequence of the more diffuse character of the

Table II. Overlaps of Selected Orbitals of Two Metal over Metal MPc (M = Co, Ni, Cu) Monomeric Units in Eclipsed ($\phi = 0°$) and Staggered ($\phi = 40°$) Configuration[a]

	$(CoPc)_2$ M–M = 3.12 Å		$(NiPc)_2$ M–M = 3.24 Å		$(CuPc)_2$ M–M = 3.19 Å	
	ϕ, deg		ϕ, deg		ϕ, deg	
	0	40	0	40	0	40
$S_{2a_{1u}}$	0.098 (1.066)	0.067 (0.716)	0.086 (0.875)	0.059 (0.584)	0.091 (0.944)	0.062 (0.636)
$S_{13a_{1g}}$	0.075 (0.881)	0.075 (0.865)	0.060 (0.644)	0.060 (0.637)	0.045 (0.631)	0.045 (0.577)
S_{6e_g}	0.041 (0.423)	0.002 (0.022)	0.033 (0.371)	0.002 (0.026)	0.079 (0.810)	0.006 (0.034)

[a] The splittings of these orbitals, in electronvolts, are also given in parentheses.

3d and the shorter metal–metal distance. Although the metal–metal distance in $(CuPc)_2$ is 0.05 Å shorter than in $(NiPc)_2$, we find a smaller splitting. This reflects the smaller overlap between the $13a_{1g}$ orbitals (0.045 in $(CuPc)_2$ versus 0.060 in $(NiPc)_2$), but we also note the relatively large Pc content of the CuPc $13a_{1g}$ orbital and the stabilization of the antibonding combination of $13a_{1g}$ orbitals in the dimer by admixture of other Pc orbitals. There is another metal d valence orbital suitable for out-of-plane interaction with the neighboring molecule, the d_π that occurs mostly in $6e_g$ (CoPc and NiPc) or $4e_g$ (CuPc). However, as is shown in the interaction diagrams, the splitting of this orbital is strongly angle dependent. From the data reported in Table II it appears that the overlap of $6e_g$ in the three dimers decreases dramatically upon rotation of the monomeric units from 0 to 40°. This is a simple consequence of symmetry (the overlap is exactly zero at 45°). Thus, $6e_g$ splits in two almost degenerate levels ($1e_1$ and $2e_1$) when the dimers are in the staggered configuration, whereas it shows a sizeable broadening at $\phi = 0°$ which is largest in $(CuPc)_2$. Here, the $6e_g$ overlap is about twice that found in the nickel and cobalt dimers. Since in copper phthalocyanine this orbital has less metal character and is mainly (85%) ligand centered, this indicates that at these interplanar distances the π ligand orbitals overlap better than the d_π orbitals. The $9b_{1g}(d_{x^2-y^2})$ and $11b_{2g}(d_{xy})$ metal states, finally, do not show any broadening, due to the small overlap of these in-plane orbitals. As may be seen in the interaction diagrams of Figure 3, the dimerization raises the energy of the metal states with respect to the energy of the monomer states, particularly in the cobalt dimer. This can be interpreted as a charging effect.

The uppermost ligand state, $2a_{1u}$, is very suitable for intermolecular interactions, since it is composed from macrocycle p_π orbitals perpendicular to the molecular plane. However, the overlap of $2a_{1u}$ is heavily angle dependent, as indicated by the curve in Figure 4a where the overlap of $2a_{1u}$ is plotted as function of the staggering angle. Maximum overlap of $2a_{1u}$ between adjacent rings occurs at $\phi = 0$ and 45°, the overlap at $\phi = 40°$ being close to the maximum value. It is noteworthy that the overlap integral S_{2a1u} changes sign in passing from the eclipsed to staggered form and becomes 0 at $\phi \sim 20°$. This behavior may easily be understood from the nodal structure; see the contour plot (Figure 4b). The consequence is a completely flat $2a_{1u}$ band at $\phi \sim 20°$, whereas the maximum of dispersion is reached at the fully eclipsed and fully staggered geometries. At $\phi = 40°$ the $2a_{1u}$ band also shows a quite large broadening. The calculations by Pietro et al.[10a] on the variation of the $2a_{1u}$ bandwidth with twist angle in cofacially joined phthalocyanine polymers and more recent studies[10b] on interring overlap in dimer complexes of phthalocyanines lead to analogous results. As reported in Table II, at 40° the energy gap between the $2a_1$ and the $2a_2$ levels, which correspond to the out-of-phase (bonding) and in-phase (antibonding) combinations of $2a_{1u}$, is found to be 0.584, 0.636, and 0.716 eV for nickel, copper, and cobalt dimers, respectively. This trend correlates with the increase in the overlap between the $2a_{1u}$ orbitals of the two monomeric units, due to the decrease of the interplanar distances as we proceed from the nickel via the copper to the cobalt dimer.

As shown in the diagrams of Figure 3, owing to the differences in energy and in overlap of the monomer orbitals, the ground-state electronic structures of the three dimers, both in the eclipsed and staggered configuration, differ with respect to level ordering and occupation. In $(NiPc)_2$ the highest occupied orbital is the ligand-$2a_{1u}$-derived $2a_2$ orbital which is well above the $1a_2$ metal-d_{z^2}-derived orbital. The gap between the $2a_{1u}$ and $13a_{1g}$ levels of molecular NiPc is reflected in the $2a_2$–$1a_2$ gap in the dimer, since the splitting of $13a_{1g}$ is not substantially larger than the splitting of $2a_{1u}$. The first unoccupied level, $11b_{2g}(d_{xy})$, is fairly high in the virtual spectrum and has so little dispersion that it will not form a band that overlaps with the $2a_{1u}$ band. The upper

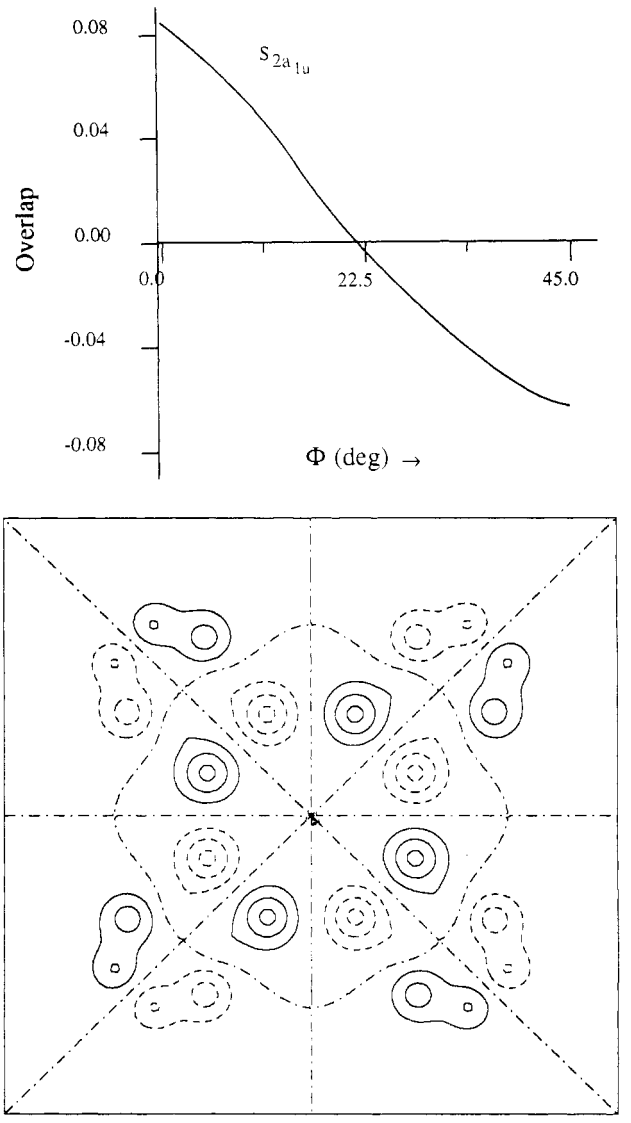

Figure 4. (a, Top) overlap of $2a_{1u}$ interacting orbitals, $S_{2a_{1u}}$, as function of the staggering angle. (b, Bottom) contour plot of the $2a_{1u}$ orbital (the orientation of the molecule is as in Figure 1). The plane of drawing is 0.7 *b* above the molecular plane. Contour values are 0.0, ±0.02, ±0.05, ±0.1, ±0.2, ±0.5 e/b^3.

part of the occupied valence band should thus consist of the broadened $2a_{1u}$ band, in complete agreement with band structure calculations by Kutzler and Ellis.[15] The relative level ordering observed at 40° holds also at 0°.

In $(CuPc)_2$, the $13a_{1g}$ orbital is so much below $2a_{1u}$ that their bands do not overlap. The $11b_{2g}(d_{xy})$ orbital is however closer now to $2a_{1u}$ than in $(NiPc)_2$. Due to the quite large splitting of $2a_{1u}$, the $2a_2$ antibonding orbital approaches the almost degenerate $11b_{2g}(d_{xy})$-derived b_1 and b_2 levels closely (to ca. 0.2 eV). In the eclipsed configuration the gap is even smaller because of the larger splitting of $2a_{1u}$. In the full band structure this implies that the flat, largely metal band arising from $11b_{2g}$ would cut through the top of the wide $2a_{1u}$ ligand band (compare the situation as calculated for Ni(tbp) by Kutzler and Ellis[15]).

In $(CoPc)_2$ it is not the unoccupied $11b_{2g}$ orbital which is close to $2a_{1u}$, but rather $13a_{1g}$ approaches $2a_{1u}$ from below closely enough that the $2a_{1u}$ and $13a_{1g}$ derived bands, both of which show considerable dispersion, overlap strongly. This fits in with the trend one expects for the relative positions of metal and Pc levels, although the singly occupied $13a_{1g}$ orbital in the CoPc monomer did not seem to conform to this expectation. The antibonding combinations of $2a_{1u}$ and $13a_{1g}$ compete in the dimer for two available electrons, and we find the triplet configuration $1a_2^1 2a_2^1$

Table III. Contributions (eV) to the Bonding Energy of $(CoPc)_2$, $(NiPc)_2$, and $(CuPc)_2$ Dimers in Eclipsed ($\phi = 0°$) and Staggered ($\phi = 40°$) Configuration, with Respect to Two MPc Monomeric Units

	$(CoPc)_2$ ϕ, deg		$(NiPc)_2$ ϕ, deg		$(CuPc)_2$ ϕ, deg	
	0	40	0	40	0	40
ΔE_{elstat}	−5.675	−2.995	−4.186	−2.243	−4.734	−2.519
ΔE_{Pauli}	+11.203	+6.322	+7.906	+4.526	+8.955	+5.051
$\Delta E°$	+5.528	+3.327	+3.720	+2.283	+4.221	+2.532
ΔE_{int}	−2.373	−2.080	−1.452	−1.374	−1.567	−1.479
ΔE_{total}	+3.155	+1.247	+2.268	+0.909	+2.654	+1.053

to be 0.826 and 0.157 eV more stable than the $1a_2^0 2a_2^2$ and $1a_2^2 2a_2^0$ configurations, respectively. The ground state of the eclipsed configuration is also found to be a triplet, 0.720 and 0.553 eV more stable than the two singlet configurations mentioned above.

(b) Energy Decomposition. A comparison between the interaction diagrams for the two possible conformations of the dimers shows that, irrespective of the dimer, most of the interactions are enhanced in a fully eclipsed arrangement, compared to the staggered one, due to an improved overlap of the involved orbitals. It should be noted, however, that most of these interactions are between filled orbitals and have been referred to in the Computational and Methodological Details as four-electron two-orbital repulsion. The repulsion is larger the more effective the overlap is. One would therefore expect the staggered configuration to be more stable than the eclipsed one for all dimers. This suggestion is supported by a quantitative energy analysis of the contributions to the bonding energies of the dimers of the series, in the eclipsed and staggered geometries. The results of this analysis are provided in Table III.

According to the data reported in the first row of Table III, a rotation of 40° of the monomers induces in the dimers of the series an identical decrease of about 47% in the attractive electrostatic interaction ΔE_{elstat}. The explanation is that the staggering increases the distances between most of the atoms of the two interacting fragments, in such a way that the stabilizing interaction between the charge density of one fragment with the nuclei of the other fragment decreases significantly. As is indicated by a quantitative analysis, not reported here, of the terms which contribute to the electrostatic interaction, the positive, destabilizing electron–electron and nucleus–nucleus repulsions also decrease when the staggering angle changes from 0° to 40°, but this is not enough to prevent the net decrease of ΔE_{elstat}. The trend shown by ΔE_{elstat} in the series suggests a strong dependence of this term on the interplanar spacing. The values reported in Table III show, in fact, that this term is largest in the cobalt dimer, where the interplanar spacing is shortest.

Looking at the Pauli repulsion term, ΔE_{Pauli} we note that, apart from the differences among the dimers in the absolute value, this term is reduced by about 43% upon variation of the rotation angle from 0° to 40°. This is understable in terms of a decrease of the overlap between most of the occupied orbitals on the interacting fragments. The Pauli repulsion term is strongly positive in all of the three dimers, however it is largest in $(CoPc)_2$ due again to the shortening of the interplanar spacing that results in larger overlaps of the orbitals on the fragments. It should be noted that, although the Pauli repulsion decreases when the dimers are in the staggered conformation, it is still rather strong. A contribution to this residual Pauli repulsion in the staggered conformation will come from the repulsion between the fully occupied $2a_{1u}$ orbitals, that overlap in both the eclipsed and staggered conformations.

ΔE_{Pauli} and ΔE_{elstat} change in opposite directions upon changing the rotation angle, but ΔE_{Pauli} is both larger in an absolute sense and has a larger variation, so when ΔE_{elstat} and ΔE_{Pauli} are combined into the steric interaction energy $\Delta E°$ one finds that $\Delta E°$ is destabilizing (positive), both for the eclipsed and the staggered configurations, but is much smaller for the staggered configuration.

As far as the stabilizing orbital interaction term ΔE_{int} is concerned, we first note that it is little influenced by the staggering, although it is slightly more stabilizing (negative) for the eclipsed arrangement, and secondly that it gives an only moderately stabilizing contribution. This is not surprising in the light of two considerations: (i) Although the Cu- and Co-containing monomers are open-shell systems, genuine electron pair bonds, with concomittant large contributions to ΔE_{int}, are not being formed. In the copper dimer the partially occupied $11b_{2g}$ orbitals of the monomers are located primarily in the molecular plane and are not suitable for out-of-plane interaction. In cobalt, the dimerization does lead to considerable interaction between the two monomer $13a_{1g}$ orbitals and between the $2a_{1u}$ orbitals. However, as noted earlier, the overlapping of the two "bands" leads to double occupation of the two bonding combinations and single occupation of the two antibonding combinations. Thus we are dealing with three-electron two-orbital interactions. In such cases the antibonding contribution most of the time largely cancels the bonding contribution. Indeed, ΔE_{int} is clearly larger in $(CoPc)_2$ than in the Ni and Cu analogues, but not by a large amount. (ii) Charge-transfer and polarization processes are not very effective since, as shown in Figure 2, the virtual orbitals of the interacting fragments except $7e_g$ and $11b_{2g}$ are at high energy. A population analysis reveals that only a slight charge transfer occurs from the occupied orbitals into these orbitals. Thus, many weak interactions between the rings contribute to ΔE_{int}, although we find that the largest energetic contribution does come from interactions in the E symmetry (E_g in the eclipsed dimers) owing to some mixing of the $7e_g$ virtual orbital into the e_g occupied orbitals.

According to Table III, the steric repulsion dominates over the attractive occupied/virtual orbital interaction for both arrangements of the dimers. Owing to a larger steric repulsion, the bonding energy is much more positive (repulsive) when the dimers assume a fully eclipsed arrangement. We have therefore clearly identified Pauli repulsion as the origin of the staggered configuration of adjacent phthalocyanine rings.

(c) Effect of Oxidation (Doping). The staggering diminishes the repulsion, but the results suggest that it does not provide a sufficiently effective way to relieve repulsions if the dimers are in the unoxidized form. This accounts for the slipped arrangement adopted by the undoped metallophthalocyanines. Slipping is maybe more efficient than rotation to relieve repulsion, owing to an overall decrease of the inter-ring overlaps. Band structure calculations[12] on a number of metallophthalocyanines suggest, in fact, a narrowing of the bands upon slipping. Our energy analysis also predicts that metal-over-metal stacking would be possible only at large interplanar spacings, for the eclipsed arrangement at even larger spacing than for the staggered configuration. A support to this suggestion is nicely provided by structural studies[8,40] concerning undoped cofacially joined $[M(Pc)O]_n$ materials. These systems, where the interplanar distance ranges from 3.33 to 3.87 Å, all possess a stacked arrangement with eclipsed phthalocyanine rings for the systems with large interplanar spacings ($[Ga(Pc)F]_n$,[40] $[Ge(Pc)O]_n$[8] and staggered phthalocyanine rings at smaller interplanar spacings ($[Si(Pc)O]_n$[8]).

The slipped to (metal-over-metal) stacked configuration change upon partial oxidation may be explained in terms of a relief of steric repulsion due to the partial emptying of the upper part (antibonding) of a significantly broadened, i.e. repulsive, band. For this mechanism to work, the Fermi level would have to coincide approximately with the top of such a band. In NiPc and in CuPc the $2a_{1u}$ band clearly meets the requirements. The interaction diagram of Figure 3b shows that for staggered $(NiPc)_2$ the upper part of the $2a_{1u}$ band is well above the d_{z^2} band, and we compute the first ligand-ionized state to be 1.2 eV more stable than the first metal-ionized one. This is in accordance with ESR and

(40) Wynne, K. J.; Nohr, R. S. *J. Chem. Soc., Chem. Commun.* **1981**, 1210.

Table IV. Energy Terms (eV) for the Formation of $(NiPc)_2$ Dimers out of Two Superimposed NiPc Fragments, at Different Staggering Angles

	ϕ, deg				
	0	10	20	40	45
ΔE_{elstat}	−4.186	−3.824	−3.221	−2.243	−2.176
ΔE_{Pauli}	+7.906	+7.073	+5.979	+4.526	+4.408
$\Delta E°$	+3.720	+3.249	+2.758	+2.283	+2.232
ΔE_{int}	−1.550	−1.517	−1.495	−1.348	−1.356
ΔE_{total}	+2.268	+1.732	+1.263	+0.909	+0.876

magnetic measurements[2b] which suggest that upon partial oxidation π-radicals are produced. As far as the CuPc system is concerned, the dimer calculations (Figure 3c) suggest that in the one-dimensional metal the $2a_{1u}$ band will overlap the narrow band of metal d_{xy} states. The partially emptied band may therefore well be $2a_{1u}$, in agreement with experimental evidence (the high metallic conductivity observed in this compound would not fit with a flat conduction band of metal d_{xy} states) and with our explanation for the slipped to stacked configuration change as the result of relief of $2a_{1u}$ repulsion. In CoPc the ligand $2a_{1u}$ band and the metal $13a_{1g}(d_{z^2})$ bands overlap, they are both broad and both embody considerable repulsion that will be diminished by emptying the upper parts of these bands through partial oxidation. Both bands may be involved in the conduction; we will return to this point in the Concluding Remarks.

The oxidation is not expected to modify substantially the relative stabilities of the eclipsed and staggered configurations, since the $2a_{1u}$ (and $13a_{1g}$ in the case of CoPc) repulsion is large at both 0 and 45°, as is evident from the comparable bandwidths (see Figure 3). The overlap $S_{2a_{1u}}$ in Figure 4a is indeed large at the two limiting angles, but as noted earlier, it is zero at ~22° and one may wonder why the $2a_{1u}$ repulsion is not avoided by adopting this rotation angle. This is a very relevant question in connection with the metallic behavior, since the zero bandwidth resulting at ~22° would destroy the conductivity. This question is addressed in the next section.

Pauli Repulsion and Origin of the Staggering Angle of ~40°

A quantitative energy analysis that we performed for $(NiPc)_2$ at different staggering angles (Table IV) shows that the theoretical energy minimum lies in the range 40–45°, in agreement with experiment. The interaction energy ΔE_{int} varies only little but is slightly more stabilizing at 0°, as expected from more extensive occupied/virtual orbital interaction. The ΔE_{Pauli} term is heavily angle dependent and, predominating over the counteracting ΔE_{elstat}, drives the system to a fully staggered configuration. What we found contradicts the suggestion by Diel et al.,[8] according to whom the driving force for the staggering is due to preferential, net bonding overlap between the π orbitals of the ring in the staggered conformation. Our calculations not only fully account for the observed staggering of ~40° but also clearly indicate that the staggering is primarily due to electronic factors (ΔE_{Pauli}) and not to external influences (crystal packing).

Where does the Pauli repulsion, responsible for the staggering, originate? As previously stressed, the Pauli repulsion term decreases in cobalt, nickel, and copper dimers by the same amount (cf. Table III) in going from the eclipsed to the staggered configuration. This behavior is indicative of a negligible influence of metal–metal repulsions on the observed staggering, that hence seems to be largely due to ring–ring interactions. This suggestion is further supported by the fact that partially oxidized H_2PcI[1g] exhibits the same staggering angle of ~40° as MPcI. In order to get a quantitative estimate of the contribution to the steric hindrance of metal–metal versus ring–ring repulsion, we analyzed, for a hypothetical dimer, $(Pc)_2$, built up by placing two phthalocyanine rings without the metal atoms at the same distance as in the nickel dimer (3.24 Å), the contributions to the steric repulsion (electrostatic interaction and Pauli repulsion) as function

Table V. Decomposition of the Steric Energy, $\Delta E°$, in Electrostatic, ΔE_{elstat}, and Pauli Repulsion, ΔE_{Pauli}, Terms for $(NiPc)_2$ and $(Pc)_2$ Dimeric Units at Different Staggering Angles

		ϕ, deg				
		0	10	20	40	45
ΔE_{elstat}	$(NiPc)_2$	−4.186	−3.824	−3.221	−2.243	−2.176
	$(Pc)_2$	−3.509	−3.155	−2.555	−1.531	−1.461
ΔE_{Pauli}	$(NiPc)_2$	+7.906	+7.073	+5.979	+4.526	+4.408
	$(Pc)_2$	+7.987	+7.144	+6.054	+4.555	+4.476
$\Delta E°$	$(NiPc)_2$	+3.720	+3.249	+2.758	+2.283	+2.232
	$(Pc)_2$	+4.478	+3.989	+3.499	+3.024	+3.015

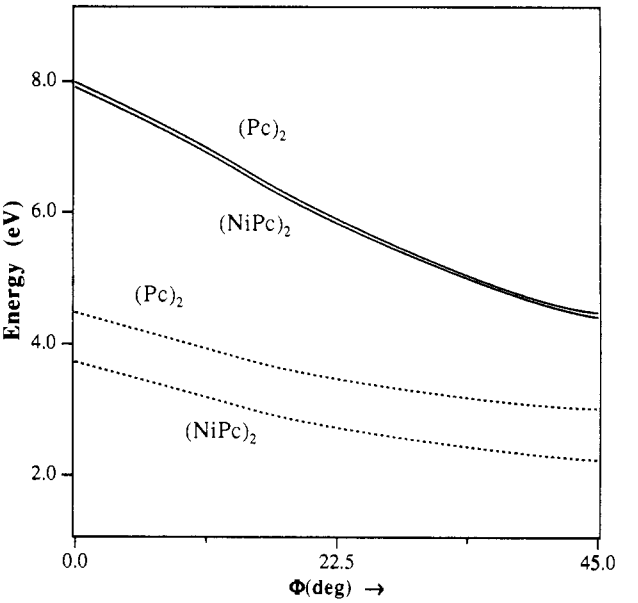

Figure 5. Pauli repulsion, ΔE_{Pauli} and steric interaction energy, $\Delta E°$, of $(NiPc)_2$ and $(Pc)_2$ dimeric units, as a function of the staggering angle.

of the staggering angle. The energy terms are reported in Table V and compared with those computed for the nickel dimer. It is interesting to note that the Pauli repulsion terms, ΔE_{Pauli}, not only show in $(Pc)_2$ and in $(NiPc)_2$ the same angle dependence but, as very clearly displayed in the plot of Figure 5, are almost identical in the two systems for all angles. The electrostatic interaction is, as expected, much smaller in $(Pc)_2$, although its angle dependence is the same in $(NiPc)_2$ and $(Pc)_2$. Thus the steric interaction term, $\Delta E°$, that is the sum of ΔE_{Pauli} and ΔE_{elstat}, is more positive (destabilizing) in the metal-free dimer than in the nickel dimer, while the $\Delta E°$ versus staggering angle curves (Figure 5) are closely parallel.

The comparison between $(NiPc)_2$ and $(Pc)_2$ unambiguously demonstrates that the Pauli repulsion originates from interactions involving *only* ligand orbitals. A contribution from the metal–metal repulsion is found only at shorter interplanar spacing. This can be inferred from the curve of Figure 6 where, for $(Pc)_2$ in the staggered conformation, ΔE_{Pauli} is plotted as a function of the distance between the rings. At the distances 3.24 and 3.19 Å, corresponding to the inter-ring distances in $Ni(Pc)_2$ and $Cu(Pc)_2$, the Pauli repulsion in $(Pc)_2$ is very close to that in the metal-containing dimers. Only at the shorter distance 3.12 Å of the $Co(Pc)_2$ dimer does the Pauli repulsion in $(Pc)_2$ notably lag behind that in the metal-containing dimer (6.072 eV versus 6.322 eV).

The relief of Pauli repulsion upon rotation must be due, then, to a decrease of the overlap of occupied ligand orbitals. With the purpose of locating these orbitals and maybe particular macrocyclic moieties responsible for steric hindrance effects, which may be important in view of the design of new macrocycles, we analyzed the overlap as a function of the staggering angle for a number of π ligand orbitals. There are indeed many occupied π ligand orbitals strongly overlapping at 0°, which may account

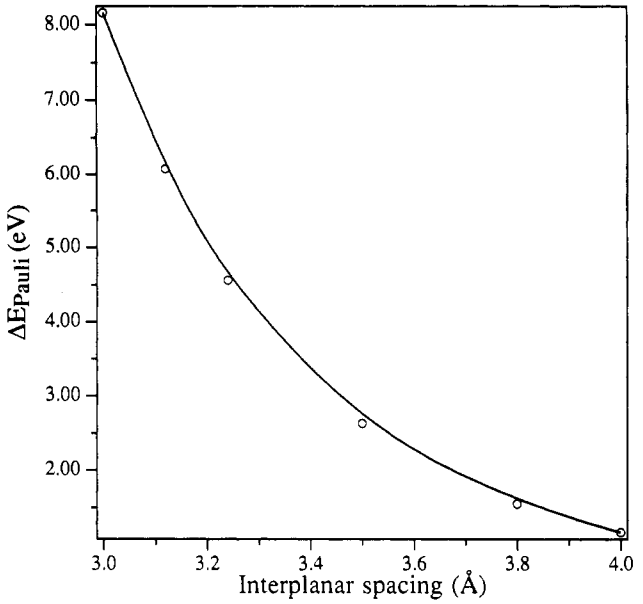

Figure 6. Pauli repulsion, ΔE_{Pauli}, between two 40° staggered Pc fragments, as a function of Pc–Pc distance.

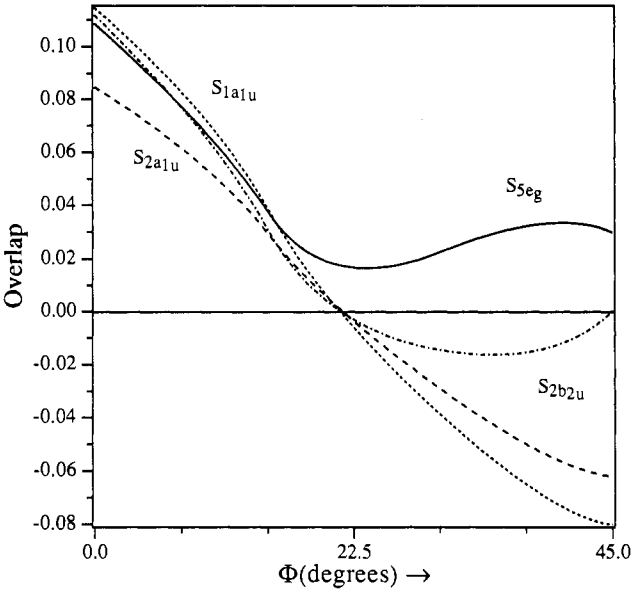

Figure 7. Overlaps of $2a_{1u}$ and lower lying π-rings orbitals as a function of the staggering angle. These orbitals show low or zero overlap at ~20°.

for the large steric repulsion observed in the fully eclipsed geometry. For many of the π ligand orbitals the overlap is strongly angle dependent, as inferred from the plots of Figures 7 and 8 where the overlaps are reported as a function of the staggering angle. The orbitals grouped in the plot of Figure 7, including the $2a_{1u}$ valence orbital, show overlap 0 at ~22° (except the $5e_g$ orbital; $2b_{2u}$ presents also a minimum at 45° and a very small overlap at ~40°). These orbitals would, in order to minimize the steric repulsion, drive the system to be rotated by ~20°. We may locate, however, a large group of low-lying π ligand orbitals, whose overlap goes down very rapidly when approaching 40–45°, as shown in the plot of Figure 8. It is noteworthy that some of these orbitals show exactly overlap 0 when the system is fully staggered, due of course to symmetry reasons.

It is quite clear then that the group of orbitals whose overlaps are shown in Figure 8 must be responsible for the staggering angle of ~40°. Interestingly, most of these orbitals are mainly located on the benzo groups, as can be inferred from the plots of Figure 9, indicating that the steric hindrance due to the benzene rings is at the origin of the staggering of ~40° observed in metallophthalocyanines and in all large-ring-based conductors.

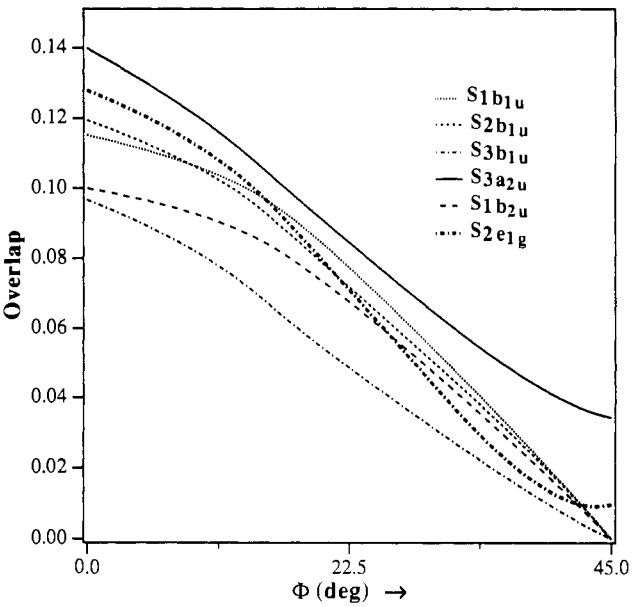

Figure 8. Overlaps of low-lying π-ligand orbitals as a function of the staggering angle. These orbitals show low overlap at ~40°.

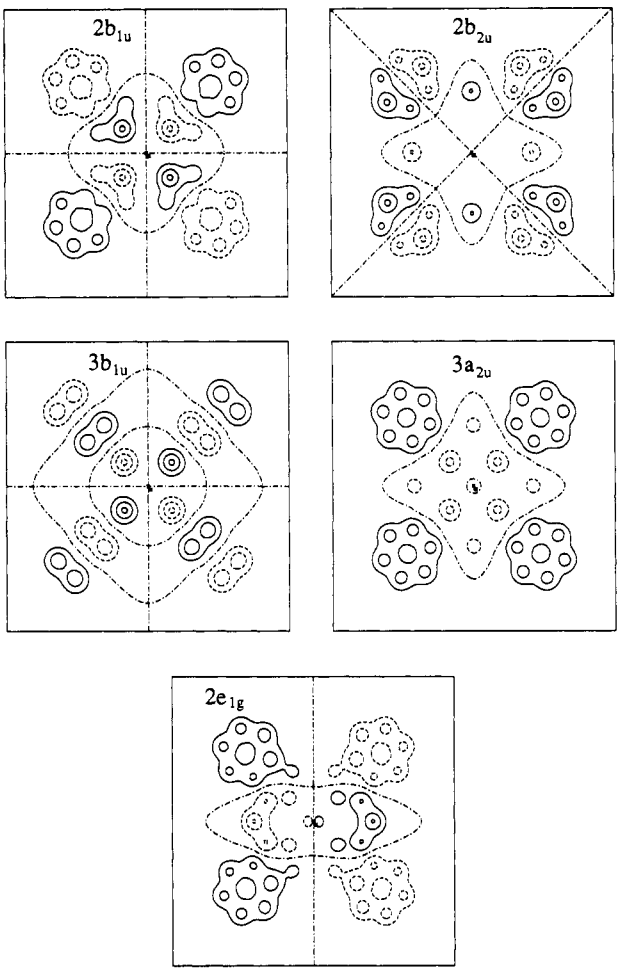

Figure 9. Contour plots of some π-ring orbitals that give large steric repulsion at 0°. These orbitals are mainly located on the benzo groups. See the caption to Figure 4b.

Concluding Remarks: Staggering and Conductivity

We have mentioned that charge transport, susceptibility, and ESR experiments show that Co(Pc)I markedly differs from Ni(Pc)I and Cu(Pc)I. The entire set of differences has been previously[2f] discussed and interpreted by treating the first as a metal-spine conductor, whereas carriers on the last two have been

associated with the Pc rings. We discuss the models for conductive pathways in the light of our theoretical results.

The oxidation process plays a primary role in determining the conductive properties of these systems and the nature of the carriers. This is demonstrated by the fact that partially oxidized metallophthalocyanines are highly conductive, while the undoped parents are known[1b,41] to present semiconducting properties. As far as Ni(Pc)I and Cu(Pc)I are concerned, our studies quite unambiguously indicate that the oxidation partially empties the $2a_{1u}$ ligand band which hence becomes the conductive band. This confirms the previous[2b,g] proposal that these compounds are π ligand conductors and that the carriers are holes. On the other hand, our theoretical results disagree with the view of Co(Pc)I as a simple metal-spine conductor.[2f] The experimental support for this view stems from some physical measurements, in particular the sign of thermoelectric power that identifies electrons as the predominant charge carriers. This is interpreted by assuming that the oxidation empties a half-occupied cobalt d_{z^2} band giving rise to a conduction band one-third filled. This picture implies, however, that a partial removal of electrons would occur from the lower part (bonding) of the d_{z^2} band. This would not account for the slipped to stacked configuration change observed upon oxidation, since removal of electrons from a half-occupied band does not relieve steric repulsion but, on the contrary, diminishes the stabilizing interaction energy. Our results indicate that the ground-state electronic structure of $(CoPc)_2$ shows an overlapping of d_{z^2} and $2a_{1u}$, with a slightly larger dispersion of the d_{z^2} band. If we would assume that the oxidation involves only the metal centers, the d_{z^2} band would be, upon oxidation, practically half-filled. Further investigation, both experimental and theoretical, will be required to establish whether Co(Pc)I is indeed a simple metal-spine conductor or that a two-band conductor model applies in this case.

We wish to emphasize that oxidation by itself, although creating a partially occupied conduction band, would not assure high conductivity if other electronic factors did not drive the system toward a stacking arrangement of the rings that enables a large dispersion of the conduction band. A large dispersion, however, implies steric repulsion if the band is fully occupied. After oxidation, which creates in, e.g., Ni(Pc)I a $2a_{1u}$ band with five-sixths occupation, some repulsion will still be present. The steric repulsion of $2a_{1u}$ and also of the other orbitals shown in the plots of Figure 7, drives the rings to $\sim 22°$. At this angle the steric repulsion due to $2a_{1u}$ is zero, but this band would have no dispersion, so the conductivity could only occur through an electron-hopping mechanism. Steric hindrance of lower π orbitals, mainly located on benzene rings, drives instead the system toward a staggering angle of 40°, and since at $\phi = 40°$ the $2a_{1u}$ band is wide, a good conductivity results.

If this argument is correct, the lack of this driving force at larger interplanar spacings or in the absence of benzo groups, would make the staggering angle move away from 40°, with dramatic consequences for the conductivity. This suggestion finds some support in experimental evidence. In Ni(omtbp),[3a] for instance, where the interplanar spacing is large (3.78 Å), the staggering angle is found to be $\sim 26°$ and the conductivity is much lower than in other large-ring-based conductors. Another interesting example is provided by the porphyrin-based conductors Ni(tmp)I, $[Ni(tmp)]_2[PF_6]$, and $[M(tmp)]_2[ReO_4]$ (M = Ni, Cu, Pd), where the conductivity is expected to be dominated by a pyrrole-ring-based a_{1u} orbital similar to $2a_{1u}$ of the M(Pc)I systems. The rotation angle is not driven to 40° by benzene rings in this case and varies in this series from 37 through 34.7 to $\sim 27°$, with a concomitant decrease in conductivity.[4e-g]

Acknowledgment. We are grateful to Mr. P. Vernooijs for his help with the calculations. A.R. is indebted to the Consiglio Nazionale delle Ricerche for a grant.

Registry No. Cobalt phthalocyanine, 3317-67-7; nickel phthalocyanine, 14055-02-8; copper phthalocyanine, 147-14-8.

(41) Berenzin, B. D. *Coordination Compounds of Porphyrins and Phthalocyanines*; Wiley: New York, 1981; p 255.